A New Family of Potent AB_5 Cytotoxins Produced by Shiga Toxigenic *Escherichia coli*

Adrienne W. Paton, Potjanee Srimanote, Ursula M. Talbot, Hui Wang, and James C. Paton

School of Molecular and Biomedical Science, University of Adelaide, South Australia, 5005, Australia

Abstract

The Shiga toxigenic *Escherichia coli* (STEC) O113:H21 strain 98NK2, which was responsible for an outbreak of hemolytic uremic syndrome, secretes a highly potent and lethal subtilase cytotoxin that is unrelated to any bacterial toxin described to date. It is the prototype of a new family of AB_5 toxins, comprising a single 35-kilodalton (kD) A subunit and a pentamer of 13-kD B subunits. The A subunit is a subtilase-like serine protease distantly related to the BA_2875 gene product of *Bacillus anthracis*. The B subunit is related to a putative exported protein from *Yersinia pestis*, and binds to a mimic of the ganglioside GM2. Subtilase cytotoxin is encoded by two closely linked, cotranscribed genes (*subA* and *subB*), which, in strain 98NK2, are located on a large, conjugative virulence plasmid. Homologues of the genes are present in 32 out of 68 other STEC strains tested. Intraperitoneal injection of purified subtilase cytotoxin was fatal for mice and resulted in extensive microvascular thrombosis, as well as necrosis in the brain, kidneys, and liver. Oral challenge of mice with *E. coli* K-12–expressing cloned *subA* and *subB* resulted in dramatic weight loss. These findings suggest that the toxin may contribute to the pathogenesis of human disease.

Key words: subtilase • enterohemorrhagic *E. coli* • serine protease • hemolytic uremic syndrome • microvascular thrombosis

Introduction

AB_5 toxins produced by pathogenic bacteria comprise an A subunit with enzymic activity and a B subunit pentamer responsible for interaction with glycolipid receptors on target eukaryotic cells (1). The three AB_5 toxin families recognized to date are the Shiga toxin (Stx), cholera toxin and the related *Escherichia coli* heat labile enterotoxins, and pertussis toxin (Ptx). In each case, they are key virulence determinants of the bacteria that produce them (Shiga toxigenic *E. coli* [STEC] and *Shigella dysenteriae*, *Vibrio cholerae*, and enterotoxigenic *E. coli*, and *Bordetella pertussis*, respectively). Collectively, these pathogens cause massive global morbidity and mortality, accounting for millions of deaths each year, particularly amongst children in developing countries. The AB_5 toxins exert their catastrophic effects by a two-step process involving B subunit–mediated entry of their respective target cells, followed by A subunit–dependent inhibition or corruption of essential host functions. The A subunits of Stx have RNA-*N*-glycosidase activity and cleave 28S rRNA, thereby inhibiting host protein synthesis. The A subunits of cholera toxin/labile enterotoxin and Ptx are ADP ribosylases that modify distinct host G proteins, resulting in alteration of intracellular cAMP levels and disregulation of ion transport mechanisms (1).

STEC are an important cause of gastrointestinal disease in humans, particularly because these infections may result in life-threatening sequelae such as the hemolytic uremic syndrome (HUS; 2, 3). STEC are a very diverse group comprising >200 *E. coli* O:H serotypes (2), but epidemiological data indicate that not all of these are highly virulent for humans. Thus, although Stx is generally considered to be a sine qua non of virulence, additional STEC properties undoubtedly contribute to the pathogenic process (2, 3). Moreover, there has been a finding of strains of *E. coli* O157:H7 and O157:H^- that do not produce Stx being associated with cases of human gastrointestinal disease, including

Address correspondence to James C. Paton, School of Molecular and Biomedical Science, University of Adelaide, South Australia, 5005, Australia. Phone: 61-8-83035929; Fax: 61-8-83033262; email: james.paton@adelaide.edu.au

Abbreviations used in this paper: aa, amino acid; CHO, Chinese hamster ovary; HUS, hemolytic uremic syndrome; IPTG, isopropyl-β-D-thiogalactopyranoside; LB, Luria-Bertani; nt, nucleotide; Ni-NTA, nickel nitrilotriacetic acid; ORF, open reading frame; Ptx, pertussis toxin; STEC, Shiga toxigenic *Escherichia coli*; Stx, Shiga toxin.

J. Exp. Med. © The Rockefeller University Press • 0022-1007/2004/07/35/12 $8.00
Volume 200, Number 1, July 5, 2004 35–46
http://www.jem.org/cgi/doi/10.1084/jem.20040392

Table I. *Bacterial Strains and Plasmids*

Bacterial strain or plasmid	Relevant characteristics	Ref. or source
E. coli		
98NK2	O113:H21 Stx2-producing STEC	5
JM109	K-12 cloning host	32
M15	expression host for pQE vectors	QIAGEN
Tuner™(DE3)	expression host for pET vectors	Novagen
DH5α^{SR}	streptomycin-resistant DH5α	33
Plasmids		
pK184		34
pQE30		QIAGEN
pET-23(+)		Novagen

HUS (4). Here, we demonstrate that certain STEC strains produce a hitherto unknown yet highly lethal AB_5 toxin. We have characterized the prototype of this new toxin family, which was secreted by a highly virulent O113:H21 STEC strain responsible for an outbreak of HUS.

Materials and Methods

Bacterial Strains, Plasmids, and Oligonucleotides. Bacterial strains, plasmids, and oligonucleotides used in this work are listed in Tables I and II. The O113:H21 STEC strain 98NK2 was isolated from a patient with HUS at the Women's and Children's Hospital, South Australia, as described previously (5). Other clinical STEC strains used in this work were also isolated at the Women's and Children's Hospital. All *E. coli* strains were routinely grown in Luria-Bertani (LB) medium (6) with or without 1.5% bacto-agar. Where appropriate, ampicillin or kanamycin were added to growth media at a concentration of 50 μg/ml.

Toxin Adsorption/Neutralization with Receptor Mimic Bacteria. *E. coli* CWG308:pJCP-Gb_3, expressing a modified lipopolysaccharide that mimics the Stx receptor Gb_3 (7) was grown overnight in LB broth supplemented with 20 μg/ml isopropyl-β-D-thiogalactopyranoside (IPTG), and 50 μg/ml kanamycin. Cells were harvested by centrifugation, washed, and resuspended in PBS at a density of 10^9 CFU/ml. 250 μl of 98NK2 culture supernatant was incubated with 500 μl of this suspension for 1 h at 37°C with gentle agitation. The mixture was centrifuged, filter sterilized, and assayed for cytotoxicity. The same procedure was also used to compare toxin neutralization using derivatives of *E. coli* CWG308 expressing mimics of Gb_4, lactoneotetraose, and GM_2 (reference 8 and unpublished data). Neutralization of cytotoxicity (%) was calculated as described previously (7).

Cell Culture and Cytotoxicity Assays. All tissue culture media and reagents were obtained from Life Technologies. Vero (African green monkey kidney) cells were grown at 37°C in DMEM supplemented with 10% heat inactivated FCS, 50 IU penicillin, and 50 μg/ml streptomycin, unless otherwise indicated. Chinese hamster ovary (CHO) cells were grown in Ham's F12 medium, whereas human colonic epithelial (Hct-8) cells were grown in RPMI 1640 medium. For cytotoxicity assays, cells were seeded into 96-well flat-bottom trays and incubated overnight at 37°C until confluent. Confluent monolayers were washed twice with PBS, treated with 50 μl of filter-sterilized toxin extracts that had been serially diluted in the appropriate tissue culture medium (without FCS), and incubated at 37°C for 30 min. After incubation, 150 μl of medium supplemented with 2% FCS was added per well. Cytotoxicity was assessed microscopically after 3 d of incubation at 37°C. The toxin titer was defined as the reciprocal of the maximum dilution producing a cytopathic effect on at least 50% of the cells in each well (CD_{50}/ml).

Manipulation and Analysis of DNA. Recombinant DNA experiments were approved by the Office of the Gene Technology Regulator (Australia) and were performed under PC2 level containment. Routine DNA manipulations (restriction digestion, agarose gel electrophoresis, ligation, transformation of *E. coli*, Southern hybridization analysis, etc.) were performed essentially as described previously (6). For DNA sequencing, a plasmid DNA template was purified using a QIAPrep Spin miniprep kit (QIAGEN). The sequence of both strands was determined using dye-terminator chemistry and either universal M13 sequencing primers or custom-made oligonucleotide primers on an automated DNA sequencer (model 3700; Applied Biosystems).

Subcloning of subAB. The *subA*, *subB*, or both *subA* and *subB* (*subAB*) open reading frames (ORFs) were amplified from 98NK2 genomic DNA by PCR using primer pairs SubAF/SubAR, SubBF/SubBR, and SubAF/SubBR, respectively, using the Expand™ High Fidelity PCR system (Roche Molecular Diagnostics), according to the manufacturer's instructions. The purified PCR products were blunt cloned into SmaI-digested pK184, and transformed into *E. coli* JM109. Recombinant plasmids were extracted from transformants and confirmed by sequence analysis. In all cases, the inserts were in the same orientation as the vector *lac* promoter.

Preparation of Antisera to SubA and SubB. To raise specific antisera, we first purified SubA and SubB using a QIAexpress kit (QIAGEN). The *subA* and *subB* ORFs, without the 5′ signal peptide-encoding regions, were amplified by high fidelity PCR using 98NK2 genomic DNA template and primer pairs pQEsubAF/pQEsubAR and pQEsubBF/pQEsubBR, respectively. Purified PCR products were digested with BamHI–SacI or SphI–SacI, respectively, ligated with similarly digested pQE30, and transformed into *E. coli* M15. Correct insertion of the genes into the vector, such that the recombinant plasmids encode derivatives of SubA and SubB with His_6 tags at their NH_2 termini, was confirmed by sequence analysis. For purification of His_6-fusion proteins, transformants were grown in 1 L of LB supplemented with 50 μg/ml ampicillin and, when the culture reached an A_{600} of 0.5, the culture was induced with 2 mM IPTG and incubated for an additional 3 h. Cells were harvested by centrifugation, resuspended in 24 ml buffer A (6 M guanidine-HCl, 0.1 M NaH_2PO_4, 10 mM Tris, pH 8.0), and stirred at room temperature for 1 h. Cell debris was removed by centrifugation at 10,000 *g* for 25 min at 4°C. The supernatant was loaded (at a rate of 15 ml/h) onto a 2 ml column of nickel nitrilotriacetic acid (Ni-NTA) resin (ProBond; Invitrogen), which had been preequilibrated with 20 ml buffer A supplemented with 0.5 M NaCl and 15 mM imidazole. The column was washed with 40 ml buffer A, followed by 20 ml buffer B (8 M urea, 0.1 M NaH_2PO_4, 10 mM Tris, pH 8.0), and 16 ml buffer C (8 M urea, 0.1 M NaH_2PO_4, 10 mM Tris, pH 6.3) supplemented with 0.25 M NaCl and 5

Table II. *Oligonucleotides*

Name	Sequence (5′–3′)
SubAF	GTACGGACTAACAGGGAACTG
SubAR	ATCGTCATATGCACCTCCG
SubBF	GTAGATAAAGTGACAGAAGGG
SubBR	GCAAAAGCCTTCGTGTAGTC
SubOLF	GGTAGCGGAACGGCAGAAGCAACAGCTATAG
SubOLR	AGCTGTTGCTTCTGCCGTTCCGCTACCAGTCC
SubAmutF	TACCCCAGTGGTCGTATCTGTTGTTGATTCCGGAGTGGCAGTGTAGGCTGGAGCTGCTTC
SubAmutR	TGTCACTTTATCTACAAGTGAAGGGTATTTATCTGCAGACCATATGAATATCCTCCTTAG
SubBmutF	TGTCTATCCCTTAATCCAGCTATGGCTGAGTGGACTGGTGGTGTAGGCTGGAGCTGCTTC
SubBmutR	ATTCTGTCGATGTGGTGCAGGTTGATAACCCAACAAGAGCACATATGAATATCCTCCTTAG
pQEsub	CCCTGGGGATCCGATGCAATTGGTCTGACAG[a]
pQEsub	GTTCGAGCTCACTCATCCTTCCCTGACG[b]
pQEsub	GGTGGCATGCGGGGGATGGCATGTTTTCAG[c]
pQEsub	CTTAGAGCTCCTTTTTCCTGTCAGGACC[b]
pETsubAF	TTGTAAGGATCCGGAGGAGCTTATGCTTAAG[a]
pETBR	GATTATCTCGAGTGAGTTCTTTTTCCTGTCAGG[d]
RTsubAF	CGAATGTTTTTCTTGCTCCAG
RTsubAR	ACACTGCTGACAGGATGATAAG
RTsubBF	GTTTTCAGGCGTTGTTATTACC
RTsubBR	CACAAAAGGTGGATACGTCC
RTsubABF	GCAGATAAATACCCTTCACTTG
RTsubABR	ATCACCAGTCCACTCAGCC

[a]Restriction site: BamHI.
[b]Restriction site: SacI.
[c]Restriction site: SphI.
[d]Restriction site: XhoI.

mM imidazole. The fusion proteins were eluted with a 30-ml gradient of 0–500 mM imidazole in buffer C, and 3-ml fractions were collected and analyzed by SDS-PAGE. Peak fractions were pooled, and the denatured SubA and SubB were refolded by dialysis against 100 ml of buffer B to which 1 L of PBS was added dropwise at a rate of 60 ml/h. This was followed by dialysis against two changes of PBS. The purified SubA and SubB were >95% pure, as judged by SDS-PAGE after staining with Coomassie brilliant blue R250.

BALB/C mice were immunized by intraperitoneal injection of three 10-μg doses of purified SubA or SubB in 0.2 ml PBS containing 5 μg of alum adjuvant (Imjectalum; Pierce Chemical Co.) at 2-wk intervals. Mice were exsanguinated by cardiac puncture 1 wk after the third immunization, and pooled antisera were stored in aliquots at −15°C.

Western Blot Analysis. Crude lysates or culture supernatants of *E. coli* strains, or purified proteins were separated by SDS-PAGE (10), and antigens were electrophoretically transferred onto nitrocellulose filters (11). Filters were probed with polyclonal mouse anti-SubA or anti-SubB sera (used at a dilution of 1:5,000), or monoclonal antibody to His_6 (QIAGEN), followed by goat anti–mouse IgG conjugated to alkaline phosphatase (Bio-Rad Laboratories). Labeled bands were visualized using a chromogenic nitro-blue tetrazolium/X-phosphate substrate system (Roche Molecular Diagnostics).

Site-directed Mutagenesis of subA. A derivative of JM109: pK184*subAB* with a point mutation such that the predicted active site serine residue (S_{271}) in SubA was altered to alanine was constructed by overlap extension PCR mutagenesis. This involved high fidelity PCR amplification of pK184*subAB* DNA using primer pairs SubAF/SubOLR and SubOLF/SubBR. This generates two fragments with the necessary mutation in codon 271 of SubA incorporated into the overlapping region by the SubOLR and SubOLF primers. The two separate PCR products were purified and mixed together, and the complete *subAB* region was reamplified using primer pair SubAF/SubBR. The resultant PCR product was blunt-cloned into SmaI-digested pK184, and transformed into *E. coli* JM109. Recombinant plasmids were purified from the resultant transformants and subjected to sequence analysis to confirm that the mutation had been introduced, and that the modified *subAB* operon was inserted in the vector in the same orientation as in pK184*subAB*. This construct was designated pK184$subA_{A271}B$.

Construction of subA and subB Deletion Derivatives of STEC 98NK2. Nonpolar *subA* and *subB* deletion mutants of STEC 98NK2 were constructed using the λ red recombinase system (12). This involved high fidelity PCR amplification of the kanamycin resistance cartridge in pKD4 using primer pairs SubAmutF/SubAmutR and SubBmutF/SubBmutR, incorporating the direct repeated FLP recognition target common priming site

and sequences derived from the 5′ and 3′ ends of the *subA* or *subB* genes, respectively. The resultant linear fragments were electroporated into 98NK2 carrying the temperature-sensitive plasmid pKD46, which encodes the λ recombinase. Allelic replacement mutants were selected on LB-kanamycin plates at 37°C. Replacement of nucleotide (nt) 169–908 of the *subA* coding sequence or nt 83–352 of *subB* with the kanamycin resistance cartridge was confirmed by PCR and sequence analysis of the mutants, which were designated 98NK2Δ*subA* and 98NK2 Δ*subB*, respectively.

RNA Extraction. RNA was extracted from log-phase LB cultures using TRIzol reagent, according to the manufacturer's instructions (Life Technologies). RNA was precipitated in 1/10 volume of sodium acetate, pH 4.8, and 2 volumes of 100% ethanol at −80°C overnight. RNA was pelleted by centrifugation at 12,000 *g* for 30 min at 4°C, washed in 70% ethanol, and resuspended in nuclease-free water. RNasein ribonuclease inhibitor (Promega) was added to the samples. Contaminating DNA was digested with RQ1 RNase-free DNase, followed by DNase stop solution, according to the manufacturer's instructions (Promega).

Real-Time RT-PCR. The comparative levels of *subA*, *subB*, and *subAB* transcripts were determined using quantitative real-time RT-PCR, using primer pairs RTsubAF/RTsubAR, RTsubBF/RTsubBR, and RTsubABF/RTsubABR, respectively. These direct amplifications of 220-bp, 238-bp, and 232-bp fragments were within *subA*, within *subB*, or spanning *subA* and *subB*, respectively. RT-PCR was performed using the one-step access RT-PCR system (Promega) according to the manufacturer's instructions. Each reaction was performed in a final volume of 20 μl, containing 20 nmol of each oligonucleotide, and a 1/20,000 dilution of Sybr green I nucleic acid stain (Molecular Probes). The quantitative RT-PCR was performed on a cycler (Rotorgene model RG-2000; Corbett Research) and included the following steps: 45 min of reverse transcription at 48°C, followed by 2 min denaturation at 94°C, and 40 cycles of amplification using 94°C for 30 s, 56°C for 30 s, and 72°C for 45 s.

Copurification of SubAB. To purify the SubAB holotoxin, the complete *subAB* coding region was amplified by high fidelity PCR using 98NK2 DNA template and the primer pair pETsubAF/pETsubBR. The resultant PCR product was digested with BamHI and XhoI, ligated with similarly digested pET-23(+), and transformed into *E. coli* Tuner™(DE3). This resulted in IPTG-dependent production of both the SubA and SubB proteins (including their respective signal peptides), but with a His_6 tag fused to the COOH terminus of SubB. Correct insertion of the genes into the vector was confirmed by sequence analysis. Cells were grown in 1 L of LB supplemented with 50 μg/ml ampicillin and, when the culture reached an A_{600} of 0.5, the culture was induced with 5 mM IPTG and incubated for an additional 3 h. Cells were harvested by centrifugation, resuspended in 20 ml of loading buffer (50 mM sodium phosphate, 300 mM NaCl, pH 8.0), and lysed in a French pressure cell. Cell debris was removed by centrifugation at 100,000 *g* for 1 h at 4°C. The supernatant was loaded onto a 2-ml column of Ni-NTA resin that had been preequilibrated with 20 ml of loading buffer. The column was washed with 40 ml wash buffer (50 mM sodium phosphate, 300 mM NaCl, 10% glycerol, pH 6.0). Bound proteins were eluted with a 30-ml gradient of 0–500 mM imidazole in wash buffer, and 3-ml fractions were collected and analyzed by SDS-PAGE.

Cross-linking of SubAB. Purified SubAB was treated with 0.5% formaldehyde for 60 min at room temperature and heated at 60°C for 10 min before SDS-PAGE analysis to determine the size of the holotoxin. Purified *E. coli* heat labile enterotoxin (unpublished data), which is known to have AB_5 stoichiometry, was treated and analyzed in parallel.

Immunofluorescence. Vero cells were grown on glass coverslips in 24-well tissue culture plates and treated with or without 1 μg/ml of purified SubAB. After 1 or 48 h, cells were fixed with 4% formaldehyde in PBS for 10 min, and in some cases permeabilized with 0.1% Triton X-100. Coverslips were washed in PBS and blocked with 20% FCS in PBS for 1 h at 37°C. They were treated with either anti-SubA, anti-SubB, or nonimmune mouse serum (diluted 1:800 in PBS/10% FCS) for 2 h at 37°C. After three washes with PBS, the coverslips were reacted with goat anti–mouse IgG–ALX488 conjugate (Molecular Probes), diluted 1:250 in PBS/10% FCS, for 30 min at 37°C. The coverslips were washed three times with PBS, twice with water, dried, and mounted on glass slides using 3 μl of Mowiol solution with antibleach. Slides were examined with a microscope (model IMT-2; Olympus) equipped with epifluorescence optics, using a 60× oil-immersion apochromatic objective.

Distribution of subAB. Crude lysates of STEC strains were subjected to PCR amplification using primer pair RTsubABF/RTsubABR. Alternatively, HindIII digests of genomic DNA purified from the STEC strains were transferred to nylon membranes and probed at high stringency with a digoxigenin-labeled *subAB* DNA fragment obtained by PCR amplification of pK184*subAB* using primer pair subAF/SubBR.

In Vivo Studies. Animal experimentation was conducted in accordance with the Australian Code of Practice for the Care and Use of Animals for Scientific Purposes, and was approved by the Animal Ethics Committee of the University of Adelaide. Groups of eight 5–6-wk-old BALB/C mice, each weighing ∼17–19 g, were given oral streptomycin (5 mg/ml in drinking water) for 24 h before oral challenge with $\sim 10^8$ CFU of a streptomycin-resistant derivative of *E. coli* DH5α (DH5α^{SR}) carrying pK184, pK184*subAB*, or pK184*subA*$_{A271}$*B*, suspended in 60 μl of 20% sucrose and 10% $NaHCO_3$. Drinking water was supplemented with 5 mg/ml streptomycin and 100 μg/ml kanamycin. Mice were weighed daily, and numbers of the recombinant bacteria in fecal samples from each group were monitored by plating on LB agar supplemented with 50 μg/ml streptomycin and 50 μg/ml kanamycin. Alternatively, pairs of BALB/C mice were injected intraperitoneally with either 25 μg, 5 μg, 1 μg, or 200 ng purified SubAB in 0.1 ml PBS.

Anti-SubAB ELISA Assay. Antibodies to SubAB were measured by ELISA using 96-well Costar PVC plates that were coated overnight at 4°C with 100 μl of 5 μg/ml of purified SubAB in TBS (25 mM Tris-HCl, 132 mM NaCl, pH 7.5). Plates were washed with TBS-0.1% Triton X-100 and blocked with TBS-0.05% Tween-20, 0.02% BSA (TBS-Tween-BSA) for 2 h at 37°C. Plates were washed again and incubated for 4 h at 37°C with 100 μl of serial dilutions of mouse serum in TBS-Tween-BSA, commencing at 1:50. Plates were washed, incubated with goat anti–mouse IgG alkaline phosphatase conjugate (EIA grade; Bio-Rad Laboratories), and diluted 1:15,000 in TBS-Tween-BSA for 2 h at 37°C. Plates were washed and developed with 1 mg/ml p-nitrophenyl phosphate substrate (in 12.5 mM triethanolamine, 135 mM NaCl, 0.02% BSA, 1 mM $MgCl_2$, 2.5 μM $ZnCl_2$, pH 9.6) for 2 h at 37°C, after which Absorbance at 450 nm was determined. Absorbance above background was plotted against serum dilution, and the ELISA titer was defined as the reciprocal of the serum dilution resulting in an A_{450} reading of 0.2 above background.

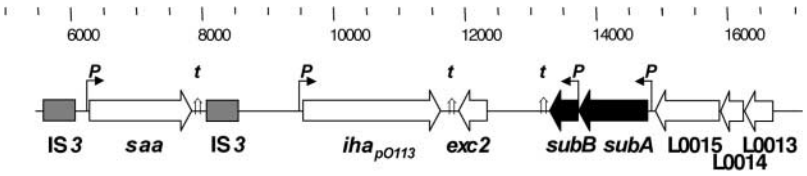

Figure 1. Map of part of the megaplasmid pO113 from 98NK2. (top) The scale indicates the corresponding nt numbers in AF399919.3. The locations of the *subA* and *subB* ORFs are shown in black arrows; other ORFs are indicated by white arrows. The gray boxes represent incomplete IS3-like elements. The locations of putative promoters (*P*) and transcription terminator sequences (*t*) are also indicated.

Results

Initial Detection of the Novel Cytotoxin. Initially, we discovered the new toxin by testing fresh culture supernatant of the O113:H21 STEC strain 98NK2 for residual cytotoxicity on Vero cells, after absorption with a recombinant *E. coli* strain that binds and neutralizes all members of the Stx family with high avidity. The latter construct expresses a modified LPS, which mimics the Stx receptor (globotriaosyl ceramide; Gb_3; reference 7). The absorbed 98NK2 supernatant exhibited significant residual cytotoxicity, with a titer of ~1,280 50% cytotoxic doses (CD_{50}) per milliliter, compared with 10,240 CD_{50}/ml for unabsorbed supernatant. A similar degree of residual cytotoxicity was also observed in supernatant from a derivative of 98NK2 with a deletion mutation in its single Stx-encoding gene (13). The cytopathic effect was maximal after 3 d of incubation and was characterized by rounding of cells, detachment from the substratum, and loss of viability (judged by Trypan blue exclusion).

Characterization of the Novel Cytotoxin Operon. To isolate the novel cytotoxin genes, we tested culture supernatants from a 98NK2 cosmid gene bank previously constructed in *E. coli* DH1 (14) for Vero cytotoxicity. Two cosmid clones with partially overlapping inserts were cytotoxic (titers were ~1,280 CD_{50}/ml). The inserts of these cosmids do not contain *stx* genes, and are derived from a 36.8-kb portion of the 98NK2 megaplasmid pO113, the sequence of which has been deposited in GenBank/EMBL/DDBJ (accession no. AF399919.3). The organization of genes within the region from nt 5,000 to 17,000 in this sequence is represented in Fig. 1. Within this region, there are two closely linked genes that we have designated *subA* and *subB*. The *subA* gene is located on the complementary strand (nt 13,725–14,768 of AF399919.3) and is preceded by a ribosome binding site (GGAGGAG; nt 14,772–14,778). A putative promoter sequence was identified using the NNPP program (15) with transcription predicted to start at nt 14,831. The *subA* gene encodes a 347–amino acid (aa) putative secreted protein with a modest degree of similarity to members of the Peptidase_S8 (subtilase) family of serine proteases (pfam00082.8). Its closest bacterial relative is the BA_2875 gene product of *Bacillus anthracis* (26% identity, 39% similarity over 246 aa). The deduced aa sequence includes a predicted signal peptide cleavage site (determined using the program SignalP V1.1; reference 16) between A_{21} and E_{22}, which was subsequently confirmed by NH_2-terminal aa sequence analysis of isolated protein. PROSITE analysis also indicated that SubA contains three conserved sequence domains, designated the catalytic triad, characteristic of members of the subtilase family (17). The SubA domain sequences match the consensus sequences for the so-called Asp, His, and Ser subtilase catalytic domains at 11/12, 10/11, and 10/11 positions, respectively, including the known active site residues (Fig. 2).

The *subB* gene is 16 nt downstream of *subA* (nt 13,283–13,708 of AF399919.3) and is preceded by a ribosome-binding site (GGAGG; nt 13,714–13,718). An additional putative promoter sequence was identified upstream of *subB* with transcription predicted to start at nt 13,774. A potential stem-loop element ($\Delta G = -19.6$ kcal/mol) located immediately downstream of *subB* (nt 13,176–13,206) may function as a transcription terminator for both *subA* and *subB* because no such elements were identified downstream of *subA*. The *subB* gene encodes a 141-aa protein with significant similarities to putative exported proteins from *Yersinia pestis* (YPO0337; 56% identity, 79% similarity over 136 aa) and *Salmonella typhi* (STY1891; 50% identity, 68% similarity over 117 aa). STY1891 has similarity (30% identity over 101 aa) to the S2 subunit of Ptx, but there is negligible similarity between SubB and the latter. Like SubA, the deduced aa sequence of SubB includes a predicted signal peptide cleavage site between A_{23} and E_{24}, which was also confirmed by NH_2-terminal analysis.

Requirement of Both subA and subB for Cytotoxicity. To examine the cytotoxicity of their products, we amplified *subA*, *subB*, or both *subA* and *subB* (*subAB*) by PCR, subcloned them into pK184, and transformed them into *E. coli* JM109. Culture supernatant of JM109:pK184*subAB* was

	Asp catalytic domain	His catalytic domain	Ser catalytic domain
	48 59	89 99	269 279
SubA	VSVV**D**SGVAFIG....**H**GTAMASLIAS....GT**S**EATAIVSG		
	*	*	*
Consensus subtilase	SxLL**D**DGLxxxD....**H**GSxVSGxLSS....GT**S**xSxPxxSA		
	T II S I N	T ITS ITA A TG	
	A VV T V H	M CA VAG A	
	I MM A M	G MGM V	
	V F F	C AC C	
	C	L	
		V	

Figure 2. Alignment of the three putative catalytic domains of SubA with the consensus sequence for Asp, His, and Ser catalytic domains of members of the subtilase family (reference 17). The numbers above the SubA fragments indicate the residue number of the terminal aas. Alternative consensus residues at a given position are shown vertically. The known active site residues in each subtilase catalytic domain (reference 17) are shown in bold type and underlined. *, SubA residues that do not match the consensus sequence.

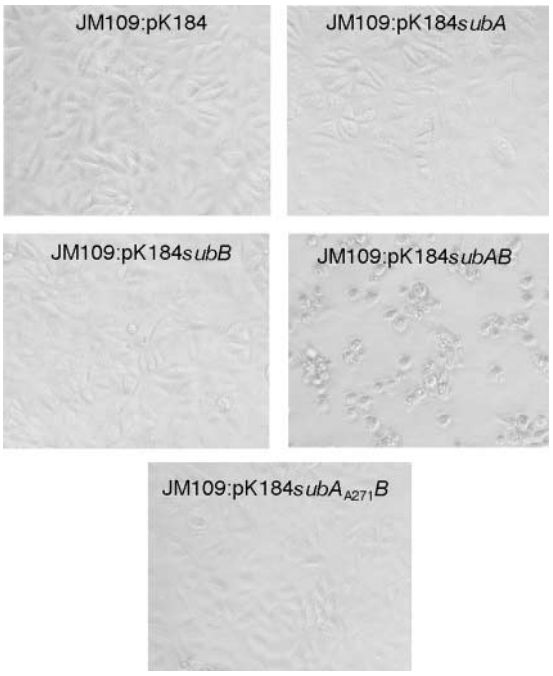

Figure 3. Cytotoxicity of SubAB for Vero cells. Monolayers were treated with 1:80 dilutions of culture supernatant from the indicated strains for 72 h and photographed under phase-contrast microscopy.

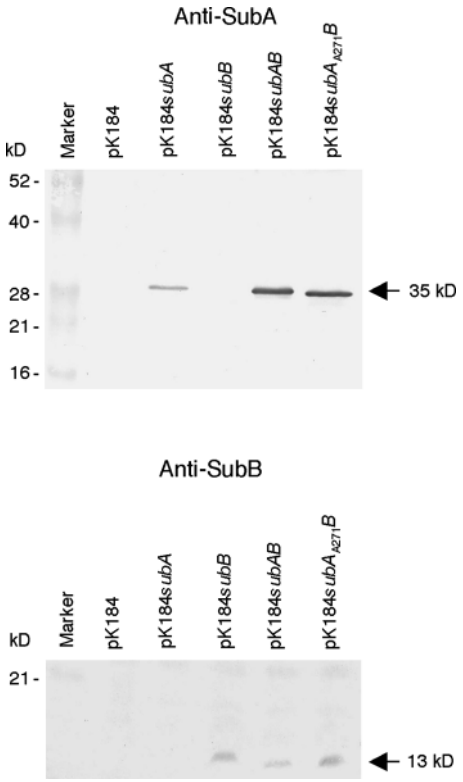

Figure 4. Western blot analysis of subclones. Culture lysates of *E. coli* JM109 carrying the indicated plasmids were separated by SDS-PAGE, electroblotted onto nitrocellulose, and probed with anti-SubA (top) or anti-SubB (bottom). The Marker track contains BenchMark prestained protein markers (Invitrogen), and the approximate sizes of visible bands are indicated on the left side of the figure. The approximate sizes of the immunoreactive species are also indicated on the right.

strongly cytotoxic for Vero cells (>40,960 CD_{50}/ml). As observed with Stx-absorbed 98NK2 culture supernatant, the cytopathic effect was maximal after 3 d of incubation and was characterized by rounding of cells, detachment from the substratum, and loss of viability (Fig. 3). However, culture supernatants of JM109:pK184*subA* and JM109:pK184*subB* were not cytotoxic (<10 CD_{50}/ml). Western blot analysis of the supernatants using polyclonal murine antisera raised against purified SubA or SubB confirmed that the appropriate clones produced immunoreactive species of the expected sizes (35 and 13 kD for SubA and SubB, respectively; Fig. 4). Cell lysates of the clones were also tested on Vero cells, and that of JM109:pK184*subAB* was at least 10 times more cytotoxic than the respective culture supernatant, which is consistent with poor release of secreted proteins from the periplasm of *E. coli* K-12 strains. CHO and Hct-8 cells were also susceptible to the JM109:pK184*subAB* culture supernatant, albeit to a lesser extent (toxin titers were 2,000 and 250 CD_{50}/ml, respectively). CHO cells are known to be refractory to Stx (18), whereas Hct-8 cells are sensitive (19).

The requirement for both *subA* and *subB* for cytotoxicity was confirmed by constructing nonpolar *subA* and *subB* deletion mutants of STEC 98NK2. Replacement of nt 169–908 of the *subA* coding sequence or nt 83–352 of the *subB* coding sequence with a 1.6-kb kanamycin resistance cassette was confirmed by PCR and sequence analysis. The resulting mutants were designated 98NK2Δ*subA* and 98NK2Δ*subB*, respectively. Western blot analysis confirmed that the former produced SubB, but not SubA, whereas the latter mutant produced SubA, but not SubB, as expected (unpublished data). The cytotoxicity of culture supernatants and cell lysates of 98NK2Δ*subA* and 98NK2Δ*subB* were examined using CHO cells, which as aforementioned, are susceptible to SubAB, but refractory to the effects of Stx. Unlike the wild-type 98NK2 extracts, those from either of the mutants had undetectable cytotoxicity. Thus, cytotoxicity requires the presence of both *subA* and *subB*.

To determine whether polyclonal murine anti-SubA or anti-SubB were capable of neutralizing toxin activity, serial dilutions of toxin were preincubated with 10-μl volumes of serum at 37°C for 30 min and assayed for residual cytotoxicity on Vero cells. No neutralization was detected using nonimmune mouse serum, but anti-SubA and anti-SubB neutralized 6,400 and 3,200 CD_{50} of toxin per ml, respectively (unpublished data).

Site-directed Mutagenesis of SubA. To determine the extent to which the cytotoxicity of SubAB was dependent on its putative subtilase activity, we constructed a derivative of JM109:pK184*subAB* with a point mutation such that the predicted active site serine residue (S_{271}) in SubA was altered to alanine. Culture supernatant from this derivative (designated JM109:pK184*subA*$_{A271}$*B*) contained both anti-SubA– and anti-SubB–reactive species of 35 and 13 kD, re-

spectively (Fig. 4). However, supernatant and cell lysate fractions from this clone exhibited markedly reduced cytotoxicity for Vero cells, with titers of 40 and 320 CD_{50}/ml, respectively (Fig. 3). Thus, the point mutation reduced specific cytotoxicity by >99.9%. Therefore, we have named the new toxin "Subtilase cytotoxin."

Transcriptional Analysis. We assessed transcription of *subA* and *subB* in 98NK2 and JM109:pK184*subAB* by real-time RT-PCR using primer pairs that direct amplification of ~230-bp fragments within *subA*, within *subB*, or spanning *subA* and *subB*. RNA templates from both strains yielded similar quantities of RT-PCR product with all three primer sets (unpublished data). This indicates that the *subA* and *subB* ORFs are cotranscribed.

Purification of the SubAB Holotoxin. The aforementioned clear requirement for both SubA and SubB for cytotoxicity strongly suggests that the two proteins function together. To examine whether they form an active complex (i.e., an AB_n holotoxin), we subcloned a DNA fragment containing the complete *subAB* region into the expression vector pET-23(+) such that a His_6 tag was fused to the COOH terminus of the expressed SubB protein. We subjected lysates of *E. coli* Tuner™(DE3) expressing this construct to Ni-NTA affinity chromatography. Proteins were eluted from the column with a 0–500-mM imidazole gradient, and fractions were analyzed by SDS-PAGE and Coomassie blue staining, as well as by Western blot using polyclonal anti-SubA or monoclonal antibody to the His_6 tag (Fig. 5). The earlier fractions (nos. 3 and 4) contained multiple protein species, including small amounts of anti-SubA–reactive material. However, all the later fractions (references 6–8 and unpublished data) contained only two protein species with sizes of 35 and 14 kD, as predicted for SubA and SubB, respectively (allowing for the extra His_6 at the SubB COOH terminus). These species reacted strongly with anti-SubA and anti-His_6, respectively. Examination of the Coomassie blue–stained SDS-PAGE gel indicated that the SubA and SubB species were present in apparently constant proportions in each of the fractions (~1:5 on a molar basis, as judged by densitometry). However, the purified SubAB migrated as a single species when subjected to PAGE under nondenaturing conditions, and was not dissociated by treatment with 5% 2-mercaptoethanol (unpublished data). Further confirmation of the stoichiometry of the association between SubA and SubB was obtained by subjecting purified SubAB to mild cross-linking conditions before SDS-PAGE analysis, which indicated that the holotoxin has a molecular size of ~105 kD (unpublished data). Collectively, these data indicate that SubA and SubB form a stable complex under nondenaturing conditions, at a ratio of 1:5.

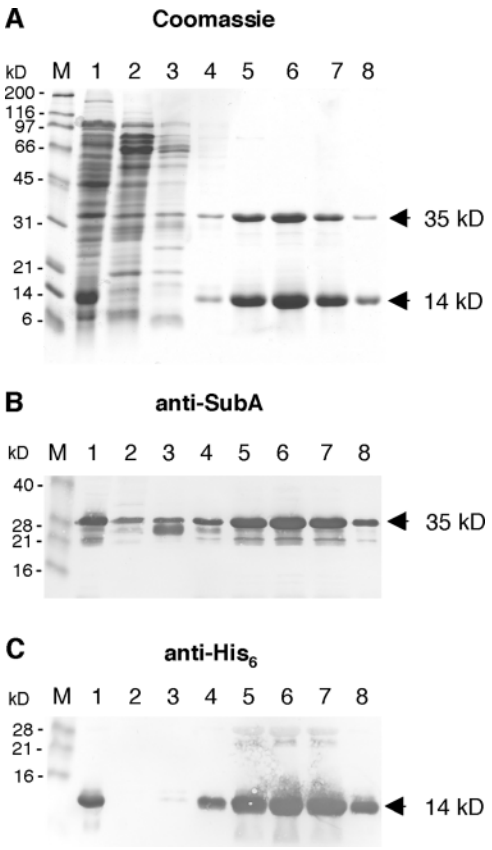

Figure 5. Copurification of SubA and SubB. Crude lysate of *E. coli* Tuner™(DE3):pET-23(+)*subAB* was applied to a Ni-NTA column, washed, and eluted with a linear 0–500-mM imidazole gradient. 10 μl aliquots of the original lysate (lane 1) and fractions 3–9 (lanes 2–8) were separated by SDS-PAGE and stained with Coomassie blue (A). Lane M contains SDS-PAGE molecular weight standards (BioRad Laboratories), and the approximate sizes are indicated on the left of the figure. Alternatively, proteins were electroblotted onto nitrocellulose and probed with polyclonal anti-SubA (B) or monoclonal anti-His_6 (C). Lane M contains BenchMark prestained protein markers (Invitrogen), and the approximate sizes of visible bands are indicated on the left side of the figure.

Cytotoxicity of Purified SubAB. Purified SubAB was highly toxic for Vero cells, with a specific activity $>10^{10}$ CD_{50}/mg. That is, <0.1 pg of SubAB is sufficient to kill at least 50% of the ~3×10^4 Vero cells present in a microtiter plate well. For comparison, the specific Vero cell cytotoxicities reported for both major Stx types (Stx1 and Stx2) are in the range of 1–10 pg/CD_{50} (20–24). Heating SubAB at 56°C for 30 min had no impact on in vitro cytotoxicity, but exposure to 75°C for 30 min resulted in ~75% inactivation (unpublished data). This degree of heat stability is similar to that reported for Stx2 (20). Like the aforementioned crude extracts tested, SubAB cytotoxicity was maximal after 72 h incubation of toxin-treated Vero monolayers, and there was little evidence of a cytopathic effect at 24 h, even at high toxin doses. Interestingly, however, if Vero cells were treated with ~1,000 CD_{50}/ml of SubAB for 60 min, followed by removal of the medium, washing of the monolayers three times with fresh medium, and continuation of incubation in fresh medium, significant cytotoxicity was still evident 48–72 h later. This suggests that significant amounts of SubAB were already either tightly bound to the Vero cell surface, or had entered the cells within the first hour.

We examined entry of SubAB into Vero cells directly, by immunofluorescence microscopy (Fig. 6). After 48-h

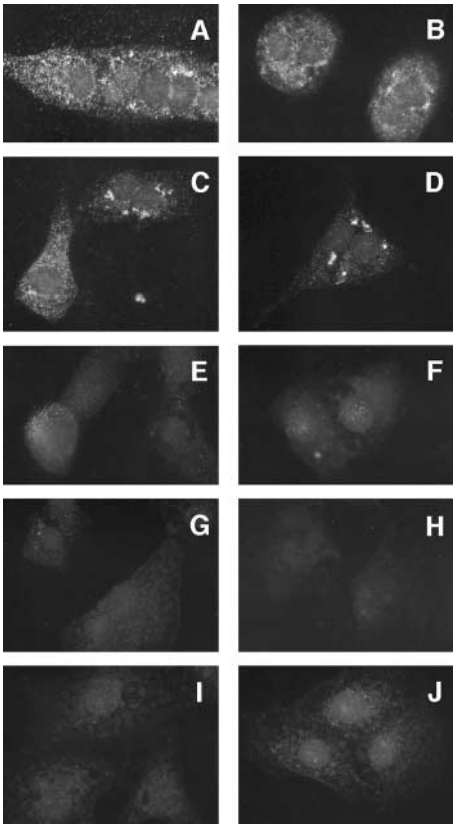

Figure 6. Immunofluorescent analysis. Vero cells were treated with purified SubAB for 48 h, fixed, permeabilized (except where indicated), and stained with mouse anti-SubA, anti-SubB, or nonimmune serum, followed by goat anti–mouse IgG-ALX488 conjugate. (A and C) Anti-SubA; (B and D) anti-SubB; (E) anti-SubA (nonpermeabilized); (F) anti-SubB (nonpermeabilized); (G) nonimmune serum; (H) nonimmune serum (nonpermeabilized); (I) anti-SubA without SubAB treatment; and (J) anti-SubB without SubAB treatment.

exposure of Vero cells to 1 μg/ml of purified SubAB, both anti-SubA– and anti-SubB–reactive material was clearly evident within the cytoplasm. No significant labeling was seen in toxin-treated cells after staining with nonimmune mouse serum, or in nontoxin-treated cells stained with the specific antisera. Furthermore, if SubAB-treated cells were not permeabilized before staining, very little immunoreactive material was observed. Thus, most of the detectable SubAB appeared to be inside the Vero cells, rather than bound to the outer surface (Fig. 6). Alternately, when toxin-treated cells were examined by immunofluorescence after only 1 h, significant staining of toxin-treated Vero cells was observed using anti-SubA or anti-SubB, regardless of whether the cells were permeabilized or not, suggesting that much of the toxin was bound to the outer surface. No labeling was observed using nonimmune mouse serum, or if Vero cells were incubated without toxin (unpublished data).

Neutralization of SubAB by a Receptor Mimic Probiotic. The B pentamers of previously characterized AB_5 toxins are known to recognize specific oligosaccharide moieties displayed by host cell glycolipids (1). Differences in receptor specificity of the toxins, as well as in the distribution of the target glycolipids between host species and tissues, has a major impact on host susceptibility and tissue tropism, and the pathology and clinical manifestations of toxin-mediated disease (25). In an attempt to identify candidate glycolipid receptors for SubAB, we absorbed toxin extracts with suspensions of recombinant *E. coli* strains expressing mimics of the oligosaccharide components of glycolipids Gb_3, Gb_4, lactoneotetraosyl ceramide, and GM2 (references 7, 8 and unpublished data). We tested the absorbed extracts for Vero cytotoxicity. No detectable neutralization of cytotoxicity was observed after absorption with any of the first three constructs, or with the host *E. coli* strain used to express the oligosaccharides. However, absorption with the GM2 mimic neutralized 93.4% of the SubAB activity. Thus, the oligosaccharide expressed by this strain (GalNAcβ[1→4]{NeuAcα[2→3]}Galβ[1→4]Glcβ−) may be a func-

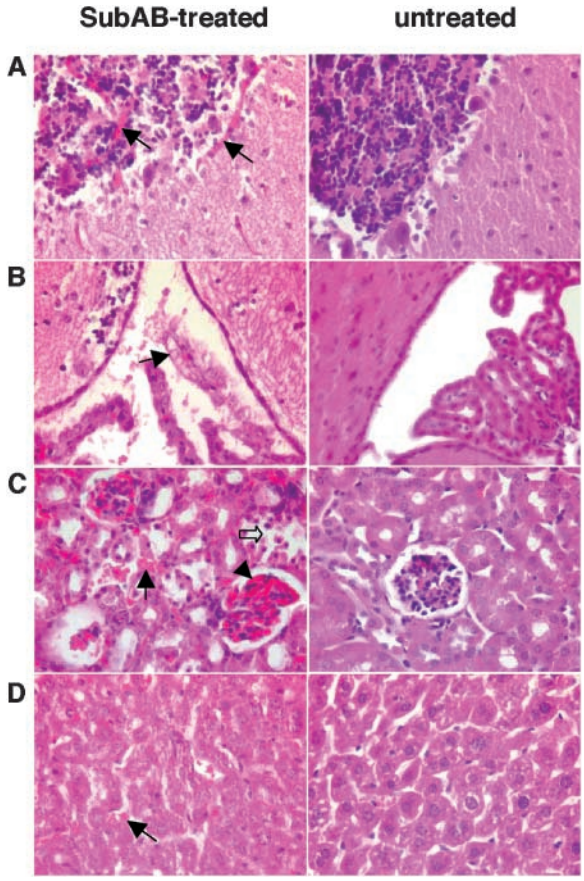

Figure 7. Histological examination of SubAB-treated mice. Mice were injected intraperitoneally with or without 1 μg of purified SubAB. After 6 d, the moribund toxin-treated mouse and the healthy control mouse were killed; brain, liver, and kidneys were removed; and fixed sections were examined histologically after staining with hematoxylin and eosin using a 40× objective. (A) Cerebellar cortex, showing hemolytic thrombi in molecular and granular layers from the toxin-treated mouse (arrows). (B) Choroid plexus, showing necrotic toxin-treated epithelial cells (arrow). (C) Renal cortex, showing interstitial thrombi (arrow), tubular necrosis (white arrow), and glomerular hyperemia (arrowhead) in the toxin-treated mouse. (D) Liver parenchyma, showing thrombi (arrow) and generalized hepatocyte necrosis in toxin-treated mouse.

tional receptor for SubAB. To examine whether Vero cells contain GM2, gangliosides were extracted and analyzed by thin layer chromatography. The extract contained at least eight species, as judged by staining with resorcinol, one of which comigrated with a commercial GM2 standard (unpublished data).

In Vivo Studies. The in vivo toxicity of SubAB was examined by intraperitoneal injection of pairs of mice with 25 μg, 5 μg, 1 μg, or 200 ng of purified toxin. All of the mice died and their survival times were inversely related to dose levels, ranging from 2 d at 25 μg to 8–10 d at 200 ng. Death was preceded by ataxia and hind limb paralysis, suggestive of neurological involvement. Histological examination of organs removed from a moribund toxin-treated mouse revealed extensive microvascular thrombosis and necrosis in the brain, liver, and kidneys (Fig. 7). One out of two mice injected with 1 μg of partially heat-inactivated (75°C for 30 min) SubAB died after 8 d, whereas the other was alive and well at 14 d.

We also challenged groups of streptomycin-treated mice orally with *E. coli* DH5α derivatives carrying pK184, pK184*subAB*, or pK184*subA*$_{A271}$*B*. The drinking water was supplemented with streptomycin and kanamycin to inhibit endogenous gut flora and to select for plasmid maintenance. Each of the constructs was maintained at levels of ~10^8–10^9 CFU/g of feces throughout the experiment. During this period, none of the mice exhibited any obvious diarrhea. The mice challenged with the control strain DH5α:pK184 or DH5α:pK184*subA*$_{A271}$*B* remained healthy and active, and gained weight steadily. By day 6, mice in these groups had gained 1.71 ± 0.21 and 1.98 ± 0.18 g, respectively. However, the mice colonized with DH5α:pK184*subAB* appeared ill and lethargic, and steadily lost body weight during the first 6 d after challenge. By day 6, they had lost 2.78 ± 0.41 g of body weight (Fig. 8 A), which is equivalent to 15.7% of their mean starting weight on day 0 (17.7 g). Even on day 3, the difference in weight gain between mice challenged with DH5α:pK184*subAB* and the other two groups was highly significant ($P < 0.01$; Student's *t* test). The severe weight loss experienced by the group challenged with the active SubAB-producing clone indicates that toxin delivered via the gut has significant deleterious effects on the host. Moreover, the fact that the growth of mice challenged with the clone expressing the SubAB protein with the mutation in the active site Ser residue was indistinguishable from that of mice challenged with DH5α:pK184 unequivocally attributes the weight loss to subtilase-mediated cytotoxic activity. Interestingly, the mice challenged with DH5α:pK184*subAB* started to gain weight from day 7, although they lagged significantly behind the other two groups for the entire duration of the experiment ($P < 0.001$; Fig. 8). To determine whether seroconversion could account for this apparent recovery, sera collected from each of the mice on day 15 were tested for antibodies to SubAB by ELISA. Only one of the mice challenged with DH5α:pK184 had detectable anti-SubAB levels, and this was at the lower limit of detection (titer = 50). However, seven out of eight mice challenged with DH5α:pK184*subAB* and five out of eight mice challenged with DH5α:pK184*subA*$_{A271}$*B* seroconverted; the highest titers for these groups were 3,100 and 720, respectively (Fig. 8 B). One out of two mice injected intraperitoneally with 1 μg of purified SubAB that had been preincubated for 1 h at 37°C with 100 μl of convalescent serum from one of the mice challenged with DH5α:pK184*subAB* died after 8 d, whereas the other was alive and well at 14 d. Preincubation of toxin with normal mouse serum had no such protective effect, with death occurring at 4 d (unpublished data).

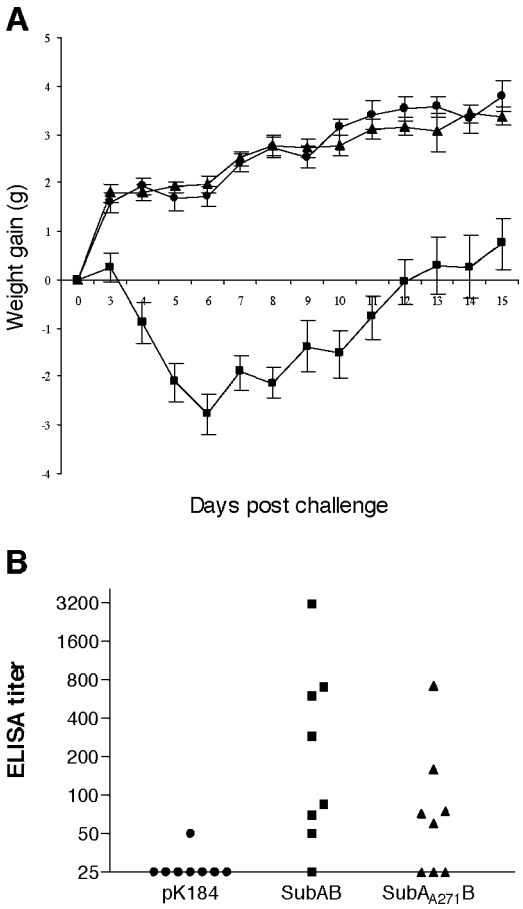

Figure 8. Oral challenge of mice with SubAB-producing clones. Groups of streptomycin-treated BALB/C mice were fed ~10^8 CFU of *E. coli* DH5α^{SR} carrying pK184 (circles), pK184*subAB* (squares), or pK184*subA*$_{A271}$*B* (triangles). Drinking water was supplemented with 5 mg/ml streptomycin and 100 μg/ml kanamycin. (A) Effect on body weight. Individually identified mice were weighed on day 0 and daily from day 3. Data are mean weight gain (± SE), relative to weight of the respective mouse on day 0. The mean weights of mice in the three groups on day 0 were 18.7, 17.8, and 18.0 g, respectively. (B) Serum anti-SubAB levels. Sera collected on day 15 were assayed for antibodies to SubAB by ELISA. The minimum detectable titer was 50, and sera below this level have been assigned a nominal titer of 25.

Distribution of subAB in Other STEC Strains. The distribution of *subAB*-related sequences in other STEC strains isolated from patients with HUS and/or diarrheal disease, or from contaminated food linked to an outbreak of HUS, was investigated by PCR and Southern hybridization anal-

Table III. *Distribution of subAB in Other STEC Serogroups*

Serogroup	No. tested	No. *subAB*$^{+a}$
O23	1	1
O26	3	0
O48	1	1
O82	1	1
O91	2	1
O98	1	0
O111	17	6
O113	5	5
O123	1	1
O128	1	1
O141	1	0
O157	15	3
O159	1	0
OX3	6	5
O nontypable	4	2
O unknown	8	5
Total	68	32

[a]Determined by PCR or Southern hybridization (see Materials and Methods).

ysis (Table III). The genes are not present in the two published O157:H7 STEC genome sequences (26, 27). However, *subAB* sequences were present in 32 out of 68 other STEC strains tested, including representatives of serogroups O23, O48, O82, O91, O111, O113, O123, O128, O157, OX3, and O nontypable strains. The *subAB* probe-reactive strains included O111:H$^-$ and O157:H$^-$ isolates linked to a large outbreak of HUS (28), and lysates of these strains were cytotoxic for (Stx resistant) CHO cells (unpublished data). The *subAB* hybridization signal obtained for the O111:H$^-$ and O157:H$^-$ isolates was not as strong as that seen for the other *subAB*-reactive strains, suggesting the possibility of sequence differences (unpublished data). All of the *subAB* positive STEC strains were also positive by PCR for the STEC enterohemolysin gene *ehxA*, which is commonly used as a marker for the presence of an STEC megaplasmid (unpublished data). The presence of *subAB* in diverse clinical isolates may be a consequence of the fact that at least in 98NK2, the operon is located on a megaplasmid (pO113) that is capable of conjugative transmission (29). However, STEC megaplasmids are heterogeneous and several of the *subAB* positive strains tested in this work have been previously shown to lack the *pilS* gene, which facilitates such transfer (29).

Discussion

In the present work, we have characterized a novel Subtilase cytotoxin at both the gene and protein level. SubAB clearly belongs in a separate family to the other AB_5 toxins characterized to date, as it has distinct A subunit enzymic activity (subtilase rather than RNA-*N*-glycosidase or ADP-ribosylase). Moreover, we have demonstrated that the potent cytotoxicity and deleterious in vivo effects of SubAB are a consequence of this subtilase activity. The subtilases are a family of serine proteases found in a wide variety of microorganisms (17, 30), but to date, no other members have been shown to have cytotoxic activity. In the present work, we also exposed Vero monolayers to 1 μg/ml purified Subtilisin Carlsberg (a prototype subtilase from *Bacillus licheniformis*; Sigma-Aldrich) and observed no cytotoxic effect whatsoever (unpublished data). SubA did not appear to have broad-spectrum proteolytic activity and was unable to cleave substrates such as collagen or fibronectin, which might have accounted for the detachment of tissue culture cells from the substratum (unpublished data). Collagen cleavage was assessed colorimetrically using dye-linked hide powder substrate, or by electrophoresis in gelatin-impregnated nondenaturing PAGE gels. Capacity to digest fibronectin was assessed by coincubation of purified human fibronectin with SubAB followed by analysis by SDS-PAGE. Immunofluorescence microscopy demonstrated that SubA and SubB bound to the surface of Vero cells within 1 h and, at 48 h, were detectable inside toxin-treated cells, but the intracellular substrate of SubA is still unknown. Nevertheless, the substrate is clearly essential for cell survival, and elucidation of this target may enable SubAB, like Ptx, to be used as a tool in cell biology.

The presence of SubB was essential for cytotoxicity, and it is likely that it is required for recognition and/or entry of target cells. The neutralization of SubAB activity achieved by treatment with the GM2 mimic probiotic suggests that this ganglioside (or one displaying a closely related oligosaccharide) may be a functional receptor for the toxin. To confirm this specificity, we attempted to neutralize SubAB with micelles of GM2 purified from bovine brain, but without success. However, the conformation of oligosaccharide moieties displayed by glycolipids in biological membranes is also heavily influenced by their own lipid component, as well as by other lipids present. This has a major impact on their capacity to interact with binding sites on AB_5 toxins (31), and purified glycolipids generally exhibit weak binding when presented in micelle form.

The evolutionary origin of Subtilase cytotoxin is unclear, but the data presented here demonstrate the potentially dire consequences that might arise from genetic rearrangements that bring seemingly innocuous genes such as *subA* and *subB* into juxtaposition. The closest bacterial homologue of SubA is BA_2875 from *B. anthracis*, but examination of the genome sequence of the latter did not reveal the presence of a gene encoding a homologue of SubB in the immediate vicinity. To our knowledge, there is also no precedent in the literature for members of the subtilase family of proteases forming stable associations with heterologous polypeptides that impact on biological activity (17, 30). Examination of the *Y. pestis* and *S. typhi* genome sequences also

did not reveal the presence of *subA*-like genes in the vicinity of their respective *subB* homologues, both of which encode products of unknown function. Nevertheless, the degree of similarity between these proteins and SubB is substantial (56% identity and 79% similarity over 136 aa in the case of *Y. pestis* YPO0337), and this raises the possibility that they are structurally and functionally related. Given the impact of plague and typhoid on human health, it would be of considerable interest to determine whether these SubB homologues can (a) form pentamers capable of binding to eukaryotic cells, and (b) interact with heterologous proteins produced by the respective organism.

The production of two distinct and highly potent AB_5 toxins (Subtilase cytotoxin and Stx) by a bacterium responsible for life-threatening human disease is an important finding that raises the possibility that both contribute (perhaps synergistically) to pathogenesis in some cases of STEC disease. Typically, the relative contributions of virulence factors can be dissected by examination of the behavior of toxin mutants in an animal model. However, existing animal models do not mimic all of the features of STEC disease in humans. Interspecies and age-related differences in receptor distribution have a major impact on host susceptibility, tissue tropism, and the resultant pathology generated by a toxin. Nevertheless, the presence of microvascular thrombi in the brain and other organs, including the renal tubules and glomeruli, of a Subtilase cytotoxin–treated mouse is suggestive of endothelial injury, and is reminiscent of the pathology seen in cases of HUS in humans. This finding is particularly intriguing in the light of the report of strains of *E. coli* O157:H7 and O157:H^- (common STEC serotypes) that do not produce Stx, being associated with HUS (4).

The presence of *subAB* in diverse STEC isolates from cases of severe human disease demands rigorous investigation of the toxin's biological effects in vitro and in vivo. The fact that *subAB* is carried on a mobile DNA element and its presence in a diverse range of *E. coli* O serogroups also raises the possibility of further transmission to other enteric bacteria. If an unequivocal role for Subtilase cytotoxin in disease in humans or animals becomes apparent, the work presented here will provide the foundation for effective diagnostic, therapeutic, and preventative strategies. We have reported PCR primers suitable for use in direct detection of *subAB*-carrying bacteria in complex clinical and environmental samples. We have demonstrated that a Ser_{271}-Ala substitution in SubA virtually abolishes cytotoxicity of SubAB, and that expression of this protein in the GI tract of mice has no adverse consequences, yet elicits a serum antibody response. Thus, we have identified a safe candidate vaccine antigen. Finally, by demonstrating that a harmless strain of *E. coli* expressing a mimic of the oligosaccharide component of ganglioside GM2 neutralizes SubAB, we have identified a means of absorbing Subtilase cytotoxin in the gut of infected individuals. Previously, we have demonstrated the in vivo efficacy of this receptor-mimic therapeutic strategy using a mimic of the Stx receptor (7).

We wish to thank L. van den Bosch and J. Cook for assistance with immunofluorescence and animal experimentation, respectively, and R. Morona and M. Jennings for helpful discussions.

This research was supported by project grant 207721 from the National Health and Medical Research Council of Australia.

Submitted: 1 March 2004
Accepted: 26 May 2004

References

1. Fan, E., E.A. Merritt, C.L.M.J. Verlinde, and W.G.J. Hol. 2000. AB(5) toxins: structures and inhibitor design. *Curr. Opin. Struct. Biol.* 10:680–686.
2. Karmali, M.A. 1989. Infection by verocytotoxin-producing *E. coli*. *Clin. Microbiol. Rev.* 2:15–38.
3. Paton, J.C., and A.W. Paton. 1998. Pathogenesis and diagnosis of Shiga toxin-producing *Escherichia coli* infections. *Clin. Microbiol. Rev.* 11:450–479.
4. Schmidt, H., J. Scheef, H.I. Huppertz, M. Frosch, and H. Karch. 1999. *Escherichia coli* O157:H7 and O157:H(-) strains that do not produce Shiga toxin: phenotypic and genetic characterization of isolates associated with diarrhea and hemolytic-uremic syndrome. *J. Clin. Microbiol.* 37:3491–3496.
5. Paton, A.W., M.C. Woodrow, R. Doyle, J.A. Lanser, and J.C. Paton. 1999. Molecular characterization of a Shiga-toxigenic *Escherichia coli* O113:H21 strain lacking *eae* responsible for a cluster of cases of hemolytic-uremic syndrome. *J. Clin. Microbiol.* 37:3357–3361.
6. Maniatis, T., E.F. Fritsch, and J. Sambrook. 1982. Molecular Cloning: A Laboratory Manual. Cold Spring Harbor Laboratory, Cold Spring Harbor, NY. 545 pp.
7. Paton, A.W., R. Morona, and J.C. Paton. 2000. A new biological agent for treatment of Shiga toxigenic *Escherichia coli* infections and dysentery in humans. *Nat. Med.* 6:265–270.
8. Paton, A.W., R. Morona, and J.C. Paton. 2001. Neutralization of Shiga toxins Stx1, Stx2c and Stx2e by recombinant bacteria expressing mimics of globotriose and globotetraose. *Infect. Immun.* 69:1967–1970.
9. Deleted in proof.
10. Laemmli, U.K. 1970. Cleavage of structural proteins during the assembly of the head of bacteriophage T4. *Nature.* 227: 680–685.
11. Towbin, H., T. Staehelin, and J. Gordon. 1979. Electrophoretic transfer of proteins from polyacrylamide gels to nitrocellulose sheets: procedure and some applications. *Proc. Natl. Acad. Sci. USA.* 76:4350–4354.
12. Datsenko, K.A., and B.L. Wanner. 2000. One-step inactivation of chromosomal genes in *Escherichia coli* K-12 using PCR products. *Proc. Natl. Acad. Sci. USA.* 97:6640–6645.
13. Rogers, T.J., A.W. Paton, S.R. McColl, and J.C. Paton. 2003. Enhanced CXC chemokine responses of human colonic epithelial cells to locus of enterocyte effacement-negative Shiga toxigenic *Escherichia coli*. *Infect. Immun.* 71:5623–5632.
14. Paton, A.W., P. Srimanote, M.C. Woodrow, and J.C. Paton. 2001. Characterization of Saa, a novel autoagglutinating adhesin produced by locus of enterocyte effacement-negative Shiga-toxigenic *Escherichia coli* strains that are virulent for humans. *Infect. Immun.* 69:6999–7009.
15. Reese, M.G., N.L. Harris, and F.H. Eeckman. 1996. Large scale sequencing specific neural networks for promoter and splice site recognition. *In* Biocomputing: Proceedings of the 1996 Pacific Symposium. L. Hunter, and T.E. Klein, editors.

World Scientific Publishing Co., Singapore.
16. Nielsen, H., J. Engelbrecht, S. Brunak, and G. von Heijne. 1997. Identification of prokaryotic and eukaryotic signal peptides and prediction of their cleavage sites. *Protein Eng.* 10:1–6.
17. Siezen, R.J., W.M. de Vos, J.A.M. Leunissen, and B.W. Dijkstra. 1991. Homology modelling and protein engineering strategy of subtilases, the family of subtilisin-like serine proteinases. *Protein Eng.* 4:719–737.
18. Jacewicz, M.S., M. Mobassaleh, S.K. Gross, K.A. Balasubramanian, P.F. Daniel, S. Raghavan, R.H. McCluer, and G.T. Keusch. 1994. Pathogenesis of *Shigella* diarrhea: XVII. A mammalian cell membrane glycolipid, Gb_3, is required but not sufficient to confer sensitivity to Shiga toxin. *J. Infect. Dis.* 169:538–546.
19. Smith, W.E., A.V. Kane, S.T. Campbell, D.W. Acheson, B.H. Cochran, and C.M. Thorpe. 2003. Shiga toxin 1 triggers a ribotoxic stress response leading to p38 and JNK activation and induction of apoptosis in intestinal epithelial cells. *Infect. Immun.* 71:1497–1504.
20. Yutsudo, T., N. Nakabayashi, T. Hirayama, and Y. Takeda. 1987. Purification and some properties of a Vero toxin from *Escherichia coli* O157:H7 that is immunologically unrelated to Shiga toxin. *Microb. Pathog.* 3:21–30.
21. Noda, M., T. Yutsudo, N. Nakabayashi, T. Hirayama, and Y. Takeda. 1987. Purification and some properties of Shiga-like toxin from *Escherichia coli* O157:H7 that is immunologically identical to Shiga toxin. *Microb. Pathog.* 2:339–349.
22. Richardson, S.E., T.A. Rotman, V. Jay, C.R. Smith, L.E. Becker, M. Petric, N.F. Olivieri, and M.A. Karmali. 1992. Experimental verocytotoxemia in rabbits. *Infect. Immun.* 60: 4154–4167.
23. Fujii, J., T. Matsui, D.P. Heatherly, K.H. Schlegel, P.I. Lobo, T. Yutsudo, G.M. Ciraolo, R.E. Morris, and T. Obrig. 2003. Rapid apoptosis induced by Shiga toxin in HeLa cells. *Infect. Immun.* 71:2724–2735.
24. Lindgren, S.W., J.E. Samuel, C.K. Schmitt, and A.D. O'Brien. 1994. The specific activities of Shiga-like toxin type II (SLT-II) and SLT-II-related toxins of enterohemorrhagic *Escherichia coli* differ when measured by Vero cell cytotoxicity but not by mouse lethality. *Infect. Immun.* 62:623–631.
25. Karlsson, K. 1998. Meaning and therapeutic potential of microbial recognition of host glycoconjugates. *Mol. Microbiol.* 19:1–11.
26. Perna, N.T., G. Plunkett III, V. Burland, B. Mau, J.D. Glasner, D.J. Rose, G.F. Mayhew, P.S. Evans, J. Gregor, H.A. Kirkpatrick, et al. 2001. Genome sequence of enterohaemorrhagic *Escherichia coli* O157:H7. *Nature.* 409:529–533.
27. Hayashi, T., K. Makino, M. Ohnishi, K. Kurokawa, K. Ishii, K. Yokoyama, C.G. Han, E. Ohtsubo, K. Nakayama, T. Murata, et al. 2001. Complete genome sequence of enterohemorrhagic *Escherichia coli* O157:H7 and genomic comparison with a laboratory strain K-12. *DNA Res.* 8:11–22.
28. Paton, A.W., R. Ratcliff, R.M. Doyle, J. Seymour-Murray, D. Davos, J.A. Lanser, and J.C. Paton. 1996. Molecular microbiological investigation of an outbreak of hemolytic uremic syndrome caused by dry fermented sausage contaminated with Shiga-like toxin-producing *Escherichia coli*. *J. Clin. Microbiol.* 34:1622–1627.
29. Srimanote, P., A.W. Paton, and J.C. Paton. 2002. Characterization of a novel type IV pilus locus carried on the large plasmid of human-virulent strains of locus of enterocyte effacement-negative Shiga-toxigenic *Escherichia coli*. *Infect. Immun.* 70:3094–3100.
30. Siezen, R.J., and J.A.M. Leunissen. 1997. Subtilases: the superfamily of subtilisin-like serine proteases. *Protein Sci.* 6:501–523.
31. Nutikka, A., and C. Lingwood. 2003. Generation of receptor-active globotriaosyl ceramide/cholesterol lipid "rafts" in vitro: A new assay to define factors affecting glycosphingolipid receptor activity. *Glycoconj. J.* 20:33–38.
32. Yanisch-Perron, C., J. Vieira, and J. Messing. 1985. Improved M13 phage cloning vectors and host strains: nucleotide sequences of the M13 mp18 and pUC19 vectors. *Gene.* 33:103–119.
33. Paton, A.W., A.J. Bourne, P.A. Manning, and J.C. Paton. 1995. Comparative toxicity and virulence of *Escherichia coli* clones expressing variant and chimeric Shiga-like toxin type II operons. *Infect. Immun.* 63:2450–2458.
34. Jobling, M.G., and R.K. Holmes. 1990. Construction of vectors with the p15a replicon, kanamycin resistance, inducible *lacZ*α and pUC18 or pUC19 multiple cloning sites. *Nucleic Acids Res.* 18:5315–5316.